Manuscript prepared for Atmos. Chem. Phys.
with version 4.2 of the LaTeX class copernicus.cls.
Date: 20 March 2014

Where do the air masses between double tropopauses come from?

Ana C. Parracho, Carlos A. F. Marques, and José M. Castanheira
CESAM, Department of Physics, University of Aveiro, Portugal
Correspondence to: J. M. Castanheira (jcast@ua.pt)

Abstract.

An analysis of the origin of air masses which are found between double tropopauses (DT) in the subtropics and midlatitudes is presented. The double tropopauses were diagnosed in the ERA-Interim reanalysis (1979–2010), and the origin of air masses was analysed using the Lagrangian model FLEXPART.

Different processes for the formation of double tropopauses (DT) have been suggested in the literature. Some studies have suggested that double tropopauses may occur as a response to the vertical profile of adiabatic heating, due to the residual meridional circulation, while others have put forward contradicting explanations. Whereas some studies have suggested that double tropopauses result from poleward excursions of the tropical tropopause over the extratropical one, others have argued that DTs develop in baroclinic unstable processes involving transport of air from high latitudes.

The results presented in this paper confirm that processes involving meridionally extended excursions of the tropical tropopause over the extratropical tropopause, which are accompanied by intrusions of air from the tropical troposphere into the lower extratropical stratosphere, make a significant contribution to the occurrence of DTs in the subtropics and midlatitudes. Specifically, it is shown that the air between double tropopauses comes from equatorward regions, and has a higher percentage of tropospheric particles and a lower mean potential vorticity. In most of the cases studied here, a layer of low static stability extends from the the tropical upper troposphere into the extratropical lower stratosphere. Moreover, the results suggest that a semipermanent character of the DT layers, in the regions where DT frequency has local maxima, is due to the overlap of the tropical and the extratropical tropopauses associated with the secondary meridional circulation involved in the jet stream dynamics.

1 Introduction

In the last 10–15 yr, several studies have focused on tropopause dynamics (see Fueglistaler et al., 2009, and Gettelman et al., 2011 for a review). In those studies two tropopause features have received special attention. One of these features, first reported by Birner (2002), consists of a strong increase of temperature with height in a layer just above the tropopause. This layer is now called the Tropopause Inversion Layer (TIL). The temperature increase in the TIL is associated with a distinct maximum in static stability parameter N^2, above which N^2 decays roughly exponentially toward typical stratospheric values (Birner, 2006). Another feature is the occurrence of double tropopause (DT) layers, i.e. layers between two levels whose thermal lapse rates satisfy the WMO (1957) definition of thermal tropopause. Double tropopauses are frequent events in the subtropics and midlatitudes (Añel et al., 2008; Castanheira and Gimeno, 2011).

The physics and dynamics that control these two features are not completely understood yet. For example, Randel et al. (2007a) and Kunz et al. (2009) suggested a radiative forcing mechanism for the TIL, whereas Birner (2010a), based on model experiments, showed that the dynamical warming due to residual stratospheric circulation is the main driver of the TIL at midlatitudes. Different explanations for the occurrence of DTs have also been suggested. Randel et al. (2007b), Pan et al. (2009) and *Homeyer et al.* (2011) presented observational evidence that double tropopause structures could result from excursions of the tropical tropopause over the extratropical tropopause, accompanied by intrusions of tropical air from the troposphere into the lower extratropical stratosphere. The results of Castanheira and Gimeno (2011) and Castanheira et al. (2012) are consistent with that mechanism. However, Wang and Polvani (2011) and Añel et al. (2012) argued that the air particles found between double tropopauses come from high latitudes, not from the tropics/subtropics. Moreover, Birner (2010a) suggests that double tropopauses in subtropics may result from a dipolar forcing (positive just above the extratropical tropopause and negative below the tropical tropopause) of the static stability by the residual circulation, a forcing also associated with the formation of the TIL.

This study is an attempt to bring out additional knowledge about the occurrence of DTs, by presenting a systematic analysis of the origin of air particles which are found between double tropopauses diagnosed in the ERA-Interim reanalysis. We analyse the backward trajectories of the particles, the potential vorticity field (PV), and the fraction of tropospheric particles found between DTs. Our results show that air masses found between double tropopauses come from regions which are equatorward (smaller latitudes and smaller PV values) of the regions from where the air masses associated with single tropopauses (STs) are found to come; and that DTs are frequently associated with tropospheric intrusions into the lower extratropical stratosphere.

Section 2 describes the data, the Lagrangian model, and the analysis method used. The main results are given in Sect. 3, and Sect. 4 closes the paper with some concluding remarks.

2 Data, Backward Trajectories, and Analysis Method

2.1 Double tropopause dataset

The first and, if present, second thermal lapse rate tropopauses were identified using the conventional WMO (1957) criteria:

a. The *first tropopause* is defined as the lowest level at which the lapse rate decreases to $2\,\mathrm{K\,km^{-1}}$ or less, provided that the average lapse rate between this level and all higher levels within $2\,\mathrm{km}$ does not exceed $2\,\mathrm{K\,km^{-1}}$.

b. If above the first tropopause the average lapse rate between any level and all higher levels within 1 km exceeds $3\,\mathrm{K\,km^{-1}}$ then a *second tropopause* is defined by the same criterion as in a. This tropopause may be either within or above the 1 km layer.

These criteria were applied to the ERA-Interim reanalysis (Dee et al., 2011) on isobaric levels using an algorithm that is similar to that used by Birner (2010b) (which in turn is a slight variation of the algorithm used by Reichler et al., 2003). The pressure fields, p_{TP}, of the first tropopause and, if present, of the second tropopause were calculated twice a day (00:00 and 12:00 UT) from 1979 to 2010, on a horizontal grid of 1.5° lat. × 1.5° long. The tropopause heights were calculated by interpolation of the geopotential heights of the two isobaric levels just above and below the tropopause pressure. A linear interpolation on the logarithm of pressure was used.

The ratio between the number of times a second tropopause is found at a given grid point and the number of times a first tropopause is calculated, in the same grid point, gives the relative frequency of DT occurrences. Figure 1 shows the frequency of DTs in the subtropics and midlatitudes of the Northern Hemisphere for the Januaries from 1979 to 2010. We analysed the month of January because the frequency of DT occurrence in the Northern Hemisphere is higher during the winter (December-February) (Añel et al., 2008; Peevey et al., 2012; Randel et al., 2007b). An analysis of a shorter 10-year period for the month of March (not discussed in the next sections) revealed results that are consistent with those obtained for January. These will be discussed in the next sections.

2.2 Backward Trajectories

The DT events occur most frequently in the latitude band of 30–40° N. To study the origin of the air which is found between DTs, 10 day back-trajectories were calculated for the 20 domains shown in Fig. 1. Eight domains were placed northward of the maxima of DT occurrence, six domains were placed along the maxima, and the remaining six domains were placed southward of the maxima of DT occurrence. These domains were chosen to sample regions with different frequencies of occurrence of DTs, and the choice of their locations was somewhat arbitrary. However, the results discussed in the following sections show that there is regional consistency between the domains, and that the conclusions would have been the same had other domains been chosen. Backward

trajectories were calculated using the 8.2 version of FLEXPART (Stohl et al., 2005), a Lagrangian Particle Dispersion Model developed at the Norwegian Institute for Air Research in the Department of Atmospheric and Climate Research, freely available at http://transport.nilu.no/flexpart.

The domains D1–D20 are boxes with horizontal dimension of 1.5° lat. × 1.5° long., centered at grid points where the STs and DTs were calculated (see Sect. 2.1). To ensure that for most cases of DT events, all particles were released between the two tropopauses, the domains' vertical boundaries (Z_1 and Z_2) were defined for each January, using the following criteria:

$$Z_1 = \overline{Z}_{TP1} + 2\sigma_{TP1} \quad (1)$$

$$Z_2 = \overline{Z}_{TP2} - \sigma_{TP2} \quad (2)$$

where $\overline{Z}_{\mathrm{TP1}}$ and $\overline{Z}_{\mathrm{TP2}}$ are the monthly mean heights of the first and second tropopause, respectively; and σ_{TP1} and σ_{TP2} are the respective monthly standard deviations. The means were calculated for each domain separately and considering only the instants with DT profiles. As may be seen from Figs. 1 and 3 of Pan et al. (2009) (and in section 3.4 of this work), a layer of extratropical stratospheric air remains just above the first tropopause, when an intrusion of tropical tropospheric air occurs. Because our simulations aim to test if the tropospheric intrusions are a main mechanism for the occurrence of DTs, we defined the lower boundary 2σ above the mean height of the first tropopause to better identify the intruded tropospheric air alone. Using the above conditions, some cases with large standard deviations may lead to domains whose thickness is smaller than $2\,\mathrm{km}$. For these cases we removed a few points most distant from the mean first tropopause and recomputed the standard deviation. Using this condition in Eqs. (1) and (2), the average thickness of the domains (boxes) is about $3.5\,\mathrm{km}$. The heights of the lower and upper boundary of each domain remained constant for all simulations in each January, and changed only from year to year to account for the variability in mean atmospheric circulation.

FLEXPART was run off-line, forced by the ERA-Interim reanalysis fields available at $6\,\mathrm{h}$ intervals (00:00 UT, 06:00 UT, 12:00 UT and 18:00 UT). In order to have forcing fields at $3\,\mathrm{h}$ intervals, the reanalysis were complemented by the fields from $3\,\mathrm{h}$ and $9\,\mathrm{h}$ forecasts at 03:00 UT, 09:00 UT, 15:00 UT and 21:00 UT. The forcing fields are available on a grid of 1° lat. × 1° long. in the 60 levels of the reanalysis model. Ten-day back trajectories were initialized twice a day, for every month of January, between 1980 and 2010. For each run, 2000 particles were released in each domain during $6\,\mathrm{h}$ time intervals centered around 00:00 and 12:00 UT.

The subroutine *calcpar.f* in FLEXPART calculates the tropopause height. However, the algorithm used to compute the tropopause in the downloaded version of FLEXPART does not implement the WMO criterion (a) for the definition of the tropopause completely. The downloaded version of *calcpar.f* tests the lapse rate criterion between two levels which are $2\,\mathrm{km}$ apart but it does not verify if the average lapse rate does not exceed $2\,\mathrm{K\,km^{-1}}$ for all levels inside the $2\,\mathrm{km}$ layer. Birner (2010b) showed that the tropopause level in the subtropics is very sensitive to the different ways the thickness criterion is implemented. Because DTs frequently occur in the subtropics, we changed *calcpar.f* in

order to implement the thickness criterion described in Sect. 2.1, i.e. the new version of subroutine *calcpar.f* verifies if the average lapse rate does not exceed $2\,\mathrm{K\,km^{-1}}$ for all levels inside the $2\,\mathrm{km}$ layer.

2.3 Analysis Method

Output variables from FLEXPART runs were recorded at $3\,\mathrm{h}$ intervals. Here, we analyse the plume centroid position coordinates (horizontal position of the center of mass of the particles released in each domain, hereafter the centroid trajectory), the mean of the potential vorticity estimated from the reanalysis fields at the position of each particle at each recorded time, and the fraction of tropospheric particles (the fraction of particles found below the first or single tropopauses).

The statistics of these variables were analysed separately for the cases of DT and ST events which were defined using the first and second tropopause heights computed from ERA-Interim data as described in Sect. 2.1. Consider a domain Di centered in the point (i,j) of the 1.5° lat. × 1.5° long. grid used to construct the DT dataset. Single tropopause events, for a domain Di, were determined using the following conditions:

1. The thermal profiles at the central point (i,j) and at the grid points $(i-1,j)$, $(i,j-1)$, $(i+1,j)$ and $(i,j+1)$ have single thermal tropopauses, at the central instant t (00:00 or 12:00 UT) of the interval for the release of the particles.

2. Let $Z_{\mathrm{ST}}(t,n)$ be the mean height of the single tropopauses in the five points, at the instant t of the nth year. Instant t is retained as a ST event, for domain Di, if

$$Z_{\mathrm{ST}}(t,n) \leq Z_1(n,\mathrm{Di}), \tag{3}$$

   where $Z_1(n,\mathrm{Di})$ is the lower boundary of Di at the nth year.

   This condition ensures that only the cases where the tropopause height is below the lower boundary of Di were retained in the analysis.

Double Tropopause events must verify the following conditions:

1. The thermal profiles at the central point (i,j) and at grid points $(i-1,j)$, $(i,j-1)$, $(i+1,j)$ and $(i,j+1)$ have multiple thermal tropopauses, at the central instant t (00:00 or 12:00 UT) of the interval for the release of the particles.

2. Let $Z_{\mathrm{DT1}}(t,n)$ and $Z_{\mathrm{DT2}}(t,n)$ be the mean heights of the first and second tropopauses in the five points, at the instant t of the nth year. Instant t is retained as a DT event, for domain Di, if the following conditions are met:

$$Z_{\mathrm{DT1}}(t,n) \leq Z_1(n,\mathrm{Di}) \tag{4}$$

$$Z_{\mathrm{DT2}}(t,n) \geq Z_2(n,\mathrm{Di}), \tag{5}$$

where $Z_2(n,\mathrm{Di})$ is the upper boundary of Di at the nth year.

Conditions (4) and (5) ensure that only cases in which the domain Di is between the two tropopauses were retained in the analysis. Using these conditions, a total of 11 235 ST events and 5137 DT events were retained. With less restrictive conditions, using only the central point of the domains, a larger number of events would be retained. Those less restrictive conditions were tested and the results did not change qualitatively but the differences between ST and DT statistics were somewhat smaller. Because we aim to test the importance of tropospheric intrusions for the occurrence of DTs, and because tropospheric intrusions should manifest in a region larger than the horizontal extension of the domains, we decided to use the aforementioned conditions. Moreover, those conditions help to avoid misidentification of ST cases, which may occur using only one vertical profile, due to the vertical resolution of the reanalyses.

Before beginning the analysis of the simulations, it is useful to review the concept behind the methodology used. If the tropospheric intrusions into the lower midlatitude stratosphere are an important mechanism for the occurrence of DTs, then significant fractions of tropospheric air must reach the domains in the case of DT events. To ensure that, in the absence of tropospheric intrusions, the tropospheric air must only be found below the domains, we adopted the stringent condition that the mean height of the first tropopauses, in the central point of the domain and in the four neighboring points, is smaller than the height of the domain's bottom boundary (conditions 3 and 4). To ensure that, in the presence of tropospheric intrusions, the stratospheric air above the second tropopause does not reach the domains, we used condition 5.

The domains were fixed in space for each January, and only ST and DT events with the first tropopause (or the single for STs) below the domains were retained in the analysis. If the tropospheric intrusions are not an important mechanism for the occurrence of DTs, the air above the first tropopause, in DT cases, or above the single tropopause, in ST cases, must predominantly show similar stratospheric characteristics. On the other hand, if tropospheric intrusions are an important mechanism for the occurrence of DTs, the air above the first tropopause, in DT cases, and the air above the single tropopauses, in ST cases, must show different characteristics, i.e. particles that reach the domains, in ST cases, must have stratospheric characteristics, and the particles that reach the domains, in DT cases, must show tropospheric characteristics.

In the following analysis we compare the characteristics of the air that reaches the domains in the cases of ST and DT events.

3 Results

3.1 Trajectory densities

In order to assess the spatial distributions of trajectories for ST and DT events, small $1^\circ \times 1^\circ$ bins were defined, covering the entire Northern Hemisphere. The number of times a (segment of a)

centroid trajectory fell on each bin was counted separately for DT and ST events. Then, the number of times a bin was crossed by the centroid trajectory was divided by the total number of ST or DT events (which varied with each domain), allowing for empirical estimates of the spatial probability density functions of trajectories for both ST and DT cases. Figure 2 shows the difference fields between trajectory densities for DT and ST events for nine domains (3 located northward of the maxima of DT occurrence, 3 placed along the maxima, and 3 located southward of the maxima of DT occurrence). The results for the other domains are similar and the differences are shown for 5 day back-trajectories. Because the position of the trajectories was recorded at 3 h intervals, 40 instants were recorded for each ST or DT event. Therefore, the ratio between the number of times a bin was crossed by the center of mass of the plume trajectory and the total number of ST or DT events gives a density normalized to 40. The horizontal projections of the centroid trajectories, for all domains shown in Fig. 2 (and also for the domains that are not shown), show that the air found between double tropopauses comes, on average, from lower latitudes than the air found for single tropopause cases. Although it is not shown, the density differences ($\mathrm{DT} - \mathrm{ST}$) are of same order of magnitude as the densities for the separate DT and ST events.

Figure 3 shows the tropopause height distributions for central points of the three domains over North America (domains D3, D10 and D16). The bimodality of the height distribution of the single tropopause is evident. Single tropopauses with the height around the mean height of the extratropical tropopause are more common northward of the maximum occurrence of DTs; and single tropopauses with the height around the mean height of the tropical tropopause are more common southward of the maximum occurrence of DTs.

Results in Figs. 2 and 3 support the hypothesis that double tropopause structures result from excursions of the tropical tropopause over the extratropical tropopause (Randel et al., 2007b; Pan et al., 2009; *Homeyer et al.*, 2011). However, we may observe in Fig. 1 that there are regions where the frequency of DTs is over 50 %. For those regions, the DT structure has a semipermanent character, and other processes (than the excursions of the tropical tropopause) should play an important role in their development, as proposed by Birner (2010a).

3.2 PV along the trajectories

The transition between the tropical tropopause and the extratropical tropopause varies in space and time. However, the analysis of the spatial distributions of trajectories for ST and DT events does not take this variability into consideration. A dynamical field that is sensitive to the transition between the troposphere and stratosphere, and between tropical and extratropical stratosphere is the potential vorticity. The analysis of the PV field helps to characterize the dynamical region from whence the air masses found between DTs come. To begin this analysis we must examine the climatological structure of the PV field, and in particular its characteristics near the tropopause. In order to preserve PV features coupled to the tropopause, we computed the climatology by averaging the fields with respect

to the local, time-dependent altitude of the first tropopause (Birner, 2006). To do that we proceeded as follows: consider a fixed horizontal grid point and let $PV(t,z)$ be the potential vorticity at height z with respect to sea level, and $Z_{\mathrm{TP1}}(t)$ be the height of the first tropopause at the same instant t. Then the time-average of PV in the tropopause based height is given by $\overline{\mathrm{PV}(t,z-Z_{\mathrm{TP1}}(t))}$, where the over line represents the time mean. Once the latter has been calculated, the vertical coordinate is readjusted using the time-averaged altitude of the tropopause, $\overline{Z}_{\mathrm{TP1}}$, as:

$$\overline{z} = z - Z_{\mathrm{TP1}} + \overline{Z}_{\mathrm{TP1}}. \tag{6}$$

Figure 4 shows the January climatology of the zonal-mean PV using the conventional vertical coordinates and the tropopause-based vertical coordinates. The PV climatology calculated using the tropopause-based height shows a strong PV gradient around the tropopause, with the isolines from 2 to 6 PVU (potential vorticity units) very close together. Above this region there is a minimum in the vertical gradient of PV. These features are not observed when the averaging is done with fixed altitude above the sea level.

The traditional meteorological approximation of PV is $P = (f+\zeta_\theta)(-g\partial\theta/\partial p)$, where g is the earth's gravity, f is the Coriolis parameter, θ is the potential temperature, and ζ_θ is the relative vorticity evaluated on isentropic surfaces (Hoskins et al., 1985). Because the static stability enters in the definition of PV through the factor $(-g\partial\theta/\partial p)$, the above characteristics of the PV field near the tropopause could be expected to be associated with the TIL. It is also emphasized that the isolines from 2 to 5 PVU are all very close to the extratropical tropopause, which may help to understand why different PV values for the definition of the dynamical tropopause appear in the literature.

In order to characterize the origin of the air masses found between DTs, we averaged the potential vorticity along the trajectories of all particles released in each ST or DT event, i.e. for each backward trajectory simulation we calculated the mean PV considering the positions of all particles (2000) at all 3 h time intervals (80), obtaining one mean PV value for each ST and each DT event. Then we calculated the distributions of the mean PV separately for ST and DT events. The results are qualitatively similar for all domains, and, in Fig. 5 we show the PV distributions considering all domains Di collectively. The solid curves represent PDFs estimated using the Kernel method (Silverman, 1986), with a normalized Kernel function. The density was evaluated in 100 equally spaced points that cover the range of values in each data set. Using the Kolmogorov–Smirnov test (K–S test) (Wilks, 2006) the DT and ST distributions were found to be statistically different at a significance level above 99 %.

Looking at Fig. 5, it may be observed that the air particles in DT cases come from an environment of lower PV than in the ST cases. The PV distribution for the ST cases peaks at 7.5 PVU, and 84 % of ST cases have mean PV values greater than 6 PVU, which are typical in the extratropical lower stratosphere. On the other hand, the PV distribution for the DT cases peaks at a value smaller than 5 PVU, and 56 % of DT cases have mean PV values smaller than 5 PVU, which are typical in the tropopause region or in the upper tropical/subtropical troposphere. These observations agree with

the idea that a significant fraction of double tropopause events could result from excursions of the tropical tropopause and tropical air over the extratropical tropopause (Randel et al., 2007b; Pan et al., 2009; *Homeyer et al.*, 2011).

Figure 5 shows the distribution of the mean PV of the reanalysis interpolated along the trajectories, for all instants and all particles of each simulation. To analyse the time evolution of PV along the trajectories, we calculated the trajectories densities as in Sect. 3.1 but in the longitude-PV space, which was divided into 3° longitude by 0.2 PVU bins (Fig. 6). Because of the relatively short period of the backward integrations, the diabatic effects are small and the PV along the trajectories must remain approximately constant. This is seen as a layered structure of density distribution of PV, with ST events having higher PV values than DT events, along the entire trajectories. Figure 6 confirms that, most frequently, the particles in DT cases come from an environment having lower PV than in ST cases.

3.3 Fraction of tropospheric particles

Another useful diagnostic for the origin of the air masses found between DTs is the fraction of tropospheric particles, TPf. At each instant, FLEXPART calculates the position of each particle with respect to the local tropopause, and gives the fraction, TPf, of particles below the tropopause. For each DT or ST event we averaged the fraction of tropospheric particles along the centroid trajectory. In this averaging we excluded the backward trajectory instants for which the nearest grid point to the centroid trajectory has a DT. With this approach, the ambiguity to consider a particle above or below the tropopause is avoided.

Taking the ST and DT cases separately, we calculated the distributions of the fraction of tropospheric particles for each domain. As for the PV, the distributions of TPf are qualitatively similar for every domain. Therefore Fig. 7 shows the box plots of TPf considering all domains collectively. It is evident that the composition of the air masses found between DTs has much more tropospheric air than the air masses found in the same space in the ST cases. For near a quarter of DT cases the fraction of tropospheric air found between DTs is more than one half, whereas only for 1 % of ST cases is the fraction of tropospheric air more than one half. These results agree with the works of Pan et al. (2009), Vogel et al. (2011) and *Homeyer et al.* (2011) which analysed the occurrence of double tropopauses in association with intrusion of tropical tropospheric air into the lower extratropical stratosphere.

3.4 Composites of static stability and zonal wind

Randel et al. (2007b) and Pan et al. (2009) pointed that near the subtropical jet core, where the tropopause changes altitudes, it is frequent for a narrow overlap of the tropical and the extratropical tropopauses to occur, producing narrow zonal bands of double tropopauses. They argued that such frequent overlap of tropopauses is consistent with the effect of the secondary meridional cir-

culation associated with the dynamics of upper-level frontal zones (e.g *Keyser and Shapiro*, 1986, Fig. 28). The meridional transport effect associated with these narrow excursions of the tropical tropopause over the extratropical tropopause is limited and should be distinguished from the deep (i.e., meridionally extended) intrusions, like those discussed by Pan et al. (2009).

It is therefore important to see what type of tropospheric intrusions our selected events represent, i.e., Are the selected DT events representing meridionally extended intrusions or are they mainly representing narrow zonal bands of double tropopauses aligned along the jet core? To answer this question we calculated the latitude-altitude composite means of the static stability N^2 and zonal wind along the meridian which passes through the domain centers. We also identified the latitude of the break of the tropical tropopause using the following criterion. Based on histograms like those shown in Fig 3 we defined extratropical tropopauses as tropopauses found below $13.5\mathrm{km}$ which is approximately the mean height of the $150-hPa$ level. Starting at the equator we searched for first three consecutive latitudes $lat(i), lat(i+1), lat(i+2)$ which have single extratropical tropopauses. The latitude of the point $(i-1)$ was taken to be the latitude of the tropical tropopause break.

Figures 8, 9 and 10 show the composites of the static stability and zonal wind for the same domains of Fig. 2. The composites for the other domains show characteristics similar to those in Figs. 8–10. The left (right) columns in the figures are the composites for DT (ST) cases. The black circles represent the first tropopause for each individual event, and the red circles represent the second tropopause in the equatorward side of the break of the tropical tropopause. Any DT found northward of the break of the tropical tropopause was not represented. The white circle with a cross represents the latitude and the mean height of the central point of the domain. In DT cases, in most of the domains, the static stability composites show a region of tropospheric-like stability between the two tropopauses, which extends northward the static stability values found in the upper tropical troposphere. This region of minimum stability is topped by a tropical tropopause which breaks on average at a latitude 5.3 degrees northward of the domains. In some cases the tropical tropopause extends northward of $60^{\circ}\mathrm{N}$. These features are suggestive of deep tropospheric intrusions. However, for domains D8 and D14 (as well as D13 and D20, not shown) the static stability and zonal wind composite features resemble 'Shapiro-like' tropopause folds (*Shapiro*, 1980). For these domains (D8, D13, D14 and D20), the break of the tropical tropopause occurs close to the jet core, whereas for the remaining domains the tropopause break occurs further north of the jet core. On average, for domains D8, D13, D14 and D20 the break occurs 7° north of the core jet, whereas for the remaining domains the break occurs 16° north of the jet core.

In the ST cases (right columns of Figs. 8–10) there is no meridionally extended minimum of static stability between the upper tropical troposphere and the lower extratropical stratosphere, and the break of the tropical tropopause occurs over the region of the jet. Roughly, for ST cases, the tropical tropopause breaks 3.5° north of jet core.

It is noteworthy that the composites show that the TIL and DTs are distinct features. In fact, for

all domains the TIL is similar for DT and ST cases. Moreover the maximum strength of the TIL occurs northwards of the domains, and for ST composites (i.e., when ST profiles occur in the domain region), the relative frequency of DTs, in region of maximum strength of the TIL, is very small. In ST composites, the relative frequency of DTs, which may occur outside the domains, is maximum in the northward flank of the jet and is consistent with the effect of the secondary meridional circulation associated to the dynamics of upper-level frontal zones (*Keyser and Shapiro*, 1986).

Domains D8, D13, D14 and D20, which show DT composites similar to 'Shapiro-like' tropopauses folds, are located in the eastern Asia and Western Pacific sector, where the mean subtropical jet has maximum strength (see Fig. 1). In these domains, for both DT and the ST composites, the DTs occur in narrow latitude band over or near the jet core. The particles that reach these domains in the ST and DT cases have less distinct potential vorticity compared with the other domains (compare Figs. 5 and 11). Therefore, a large fraction of DT events for domains D8, D13, D14 and D20 may be related to tropopauses folds. On the other hand, large fractions of DT events for the other domains seem to be associated with extended tropospheric intrusions like those discussed by Pan et al. (2009).

4 Concluding remarks

The double tropopauses (DTs) are a common feature in the subtropics and midlatitudes, especially during winter. The mechanisms behind the thermal structure of DTs are not completely understood. Birner (2010a) argued that DTs may be forced locally by the adiabatic heating associated with the meridional residual circulation. Randel et al. (2007b), Pan et al. (2009) and *Homeyer et al.* (2011) suggested that double tropopause structures could result from excursions of the tropical tropopause over the extratropical tropopause, accompanying deep (meridionally extended) intrusions of tropical tropospheric air into the lower extratropical stratosphere. However, Wang and Polvani (2011) and Añel et al. (2012) argued that the air particles found between double tropopauses come from high latitudes, not from the tropics/subtropics.

Even if, for some regions, DT structures have a semipermanent character which cannot be explained only by deep intrusions of tropical tropospheric air into the lower extratropical stratosphere, like those studied by Pan et al. (2009) and *Homeyer et al.* (2011), this mechanism should be important for the occurrence of DTs, as was also suggested recently by Castanheira and Gimeno (2011), Castanheira et al. (2012) and Peevey et al. (2012). To explain the apparent contradiction with the results of Wang and Polvani (2011) and Añel et al. (2012), we performed a systematic analysis of the origin of the air found between DTs using the Lagrangian model FLEXPART. The analysis was done for every January, from 1980 to 2010. Our results show that the air masses found between double tropopauses come from regions which are equatorward (smaller latitudes) of the regions from whence the air masses associated with STs come from. The analysis of the PV reveals that, in DT cases, the air masses come from a PV environment typical of the tropopause region and the up-

per tropical/subtropical troposphere, whereas, in ST cases, the air masses come mostly from a PV environment typical of the lower extratropical stratosphere. Moreover, in DT cases, for more one fifth (22%) of events the air masses are predominantly composed by air particles that come from the troposphere. On the other hand, in the case of STs, in more than 98% of events the air masses are predominantly composed by air particles that come from the stratosphere.

Composite analysis of the static stability and zonal wind fields showed that, in most of the domains, a significant number of events of tropopauses overlaps must be associated with meridionally extended intrusions of tropical tropospheric air into the lower extratropical stratosphere, like those analysed by Pan et al. (2009) and *Homeyer et al.* (2011). On the other hand, in four domains, all placed in the east Asia/western Pacific sector, where the subtropical jet is stronger, the composites reveal a structure resembling 'Shapiro-like' tropopause folds (*Shapiro*, 1980). At these domains, for both DT and ST events, the tropical tropopause breaks close the jet core, and the narrow overlap of the tropopauses is consistent with the effect of the secondary meridional circulation (*Keyser and Shapiro*, 1986). Moreover, looking at Fig. 1, one sees that the centers of maximum DT frequency are placed close to the jet core, suggesting that the semipermanent character of the DT structures there may be due to the effect of the secondary meridional circulation.

In summary, the results presented in this work clearly show that processes involving excursions of the tropical tropopause over the extratropical tropopause contribute significantly to the occurrence of DTs in the subtropics and midlatitudes. The narrow overlap of tropopauses near the tropical tropopause break, which is consistent with the effect of the secondary meridional circulation, may be the reason for the maxima of DT frequencies. However, meridionally extended tropopauses overlaps, associated with intrusions of tropical tropospheric air into the lower extratropical stratosphere like those analysed by Pan et al. (2009) and *Homeyer et al.* (2011), also make an important contribution to the occurrence of double tropopause layers.

Acknowledgements. This work was partially supported by the DYNOZONE project (PTDC/CTE-ATM/105507/2008) funded by the FCT (Fundação para a Ciência e a Tecnologia, Portugal). C. A. F. Marques was supported by the FCT under grant SFRH/BPD/76232/2011.

References

Añel, J. A., Antuña, J. C., de la Torre, L., Castanheira, J. M., and Gimeno, L.: Climatological features of global multiple tropopause events, J. Geophys. Res., 113, D00B08, doi10.1029/2007JD009697, 2008.

Añel, J. A., de la Torre, L., and Gimeno, L.:. On the origin of the air between multiple tropopauses at midlatitudes, The Scientific World Journal, 2012, 191028,doi10.1100/2012/191028, 2012.

Birner, T., Dörnbrack, A., and Schumann, U.: How sharp is the tropopause at midlatitudes?, Geophys. Res. Lett., 29, 45-1–45-4, doi10.1029/2002GL015142, 2002.

Birner, T.: Fine-scale structure of the extratropical tropopause region, J. Geophys. Res., 111, D04104, doi10.1029/2005JD006301, 2006.

Birner, T.: Residual circulation and tropopause structure, J. Atmos. Sci., 67, 2582–2600, doi10.1175/2010JAS3287.1, 2010a.

Birner, T.: Recent widening of the tropical belt from global tropopause statistics: sensitivities, J. Geophys. Res., 115, D23109, doi10.1029/2010JD014664, 2010b.

Castanheira, J. M., and Gimeno, L.: Association of double tropopause events with baroclinic waves, J. Geophys. Res., 116, D19113, doi10.1029/2011JD016163, 2011.

Castanheira, J. M., Peevey, T. R., Marques, C. A. F., and Olsen, M. A.: Relationships between Brewer-Dobson circulation, double tropopauses, ozone and stratospheric water vapour, Atmos. Chem. Phys., 12, 10195–10208, doi10.5194/acp-12-10195-2012, 2012.

Dee, D. P., Uppala, S. M., Simmons, A. J., Berrisford, P., Poli, P., Kobayashi, S., Andrae, U., Balmaseda, M. A., Balsamo, G., Bauer, P., Bechtold, P., Beljaars, A. C. M., van de Berg, L., Bidlot, J., Bormann, N., Delsol, C., Dragani, R., Fuentes, M., Geer, A. J., Haimberger, L., Healy, S. B., Hersbach, H., Hólm, E. V., Isaksen, L., Kållberg, P., Köhler, M., Matricardi, M., McNally, A. P., Monge-Sanz, B. M., Morcrette, J.-J., Park, B.-K., Peubey, C., de Rosnay, P., Tavolato, C., Thépaut, J.-N., and Vitart, F.: The ERA-Interim reanalysis: configuration and performance of the data assimilation system, Q. J. Roy. Meteor. Soc., 137, 553–597, doi10.1002/qj.828, 2011.

Fueglistaler, S., Dessler, A. E., Dunkerton, T. J., Folkins, I., Fu, Q., and Mote, P. W.: Tropical tropopause layer, Rev. Geophys., 47, RG1004, doi10.1029/2008RG000267, 2009.

Gettelman, A., Hoor, P., Pan, L. L., Randel, W. J., Hegglin, M. I., and Birner, T.: The extratropical upper troposphere and lower stratosphere, Rev. Geophys., 49, RG3003, doi10.1029/2011RG000355, 2011.

Homeyer, C. R., Bowman, K. P., Pan, L. L. , Atlas, E. L., Gao, R.-S., and Campos, T. L.: Dynamical and chemical characteristics of tropospheric intrusions observed during START08, J. Geophys. Res., 116, D06111, doi:10.1029/2010JD015098, 2011.

Hoskins, B. J., McIntyre, M. E., and Robertson, A. W.: On the use and significance of isentropic potential vorticity maps, Q. J. Roy. Meteor. Soc., 111, 877–946, 1985.

Keyser, D. and Shapiro, M. A.: A review of the strucure and dynamics of upper-level frontal zones, Mon. Wea. Rev., 114, 452-459, 1986.

Kunz, A., Konopka, P., Müller, R., Pan, L. L., Schiller, C., and Rohrer, F.: High static stability in the mixing layer above the extratropical tropopause, J. Geophys. Res., 114, D16305, doi10.1029/2009JD011840, 2009.

Pan, L. L., Randel, W. J., Gille, J. C., Hall, W. D., Nardi, B., Massie, S., Yudin, V., Khosravi, R., Konopka, P., and Tarasick, D.: Tropospheric intrusions associated with the secondary tropopause, J. Geophys. Res., 114,

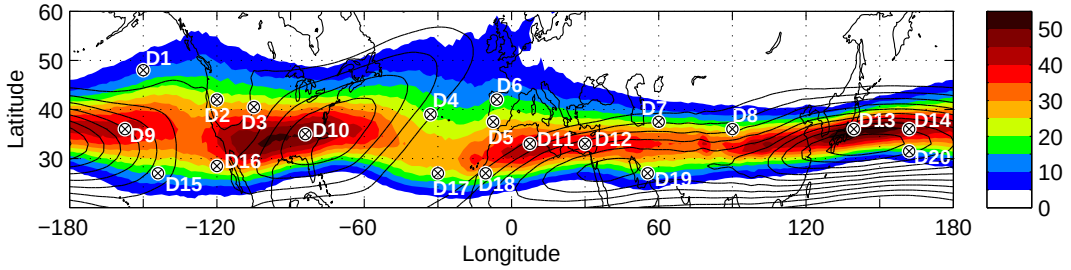

Fig. 1. Relative frequency of DT occurrences (color filled, in%) and 200-hPa mean wind speed for January (in %) overlaid with the twenty domains (D1-D20) used in this study. Contours of wind speed are represented at $5\mathrm{ms}^{-1}$ intervals, starting at $30\mathrm{ms}^{-1}$.

D10302, doi10.1029/2008JD011374, 2009.

Peevey, T. R., Gille, J. C., Randall, C. E., and Kunz, A.: Investigation of double tropopause spatial and temporal global variability utilizing high resolution dynamics limb sounder temperature observations, J. Geophys. Res., 117, D01105, doi10.1029/2011JD016443, 2012.

Randel, W. J., Wu, F., and Forster, P.: The extratropical tropopause inversion layer: global observations with GPS data, and a radiative forcing mechanism, J. Atmos. Sci., 64, 4489–4496, 2007a.

Randel, W. J., Seidel, D. J., and Pan, L. L.: Observational characteristics of double tropopauses, J. Geophys. Res., 112, D07309, doi10.1029/2006JD007904, 2007b.

Reichler, T., Dameris, M., and Sausen, R.: Determining the tropopause height from gridded data, Geophys. Res. Lett., 30, 2042, 2003.

Shapiro, M. A.: Turbulent mixing within tropopause folds as a mechanism for exchange of chemical constituents between the stratosphere and troposphere. J. Atmos. Sci., 37, 994-1004, 1980.

Silverman, B. W.: Density Estimation for Statistics and Data Analysis, Chapman and Hall, London, 175 pp., 1986.

Stohl, A., Forster, C., Frank, A., Seibert, P., and Wotawa, G.: Technical note: The Lagrangian particle dispersion model FLEXPART version 6.2, Atmos. Chem. Phys., 5, 2461–2474, doi10.5194/acp-5-2461-2005, 2005.

Vogel, B., Pan, L. L., Konopka, P., Gunther, G., Muller, R., Hall, W., Campos, T., Pollack, I., Weinheimer, A., Wei, J., Atlas, E. L., and Bowman, K. P.: Transport pathways and signatures of mixing in the extratropical tropopause region derived from Lagrangian model simulations, J. Geophys. Res., 116, D05306, doi10.1029/2010JD014876, 2011.

Wang, S. and Polvani, L. M.:, Double tropopause formation in idealized baroclinic life cycles: the key role of an initial tropopause inversion layer, J. Geophys. Res., 116, D05108, doi10.1029/2010JD015118, 2011.

Wilks, D. S.: Statistical Methods In Atmospheric Sciences, Elsevier, San Diego, California, USA, 649 pp., 2006.

World Meteorological Organization: Meteorology: A three-dimensional science, WMO Bull., 6, 134–138, 1957.

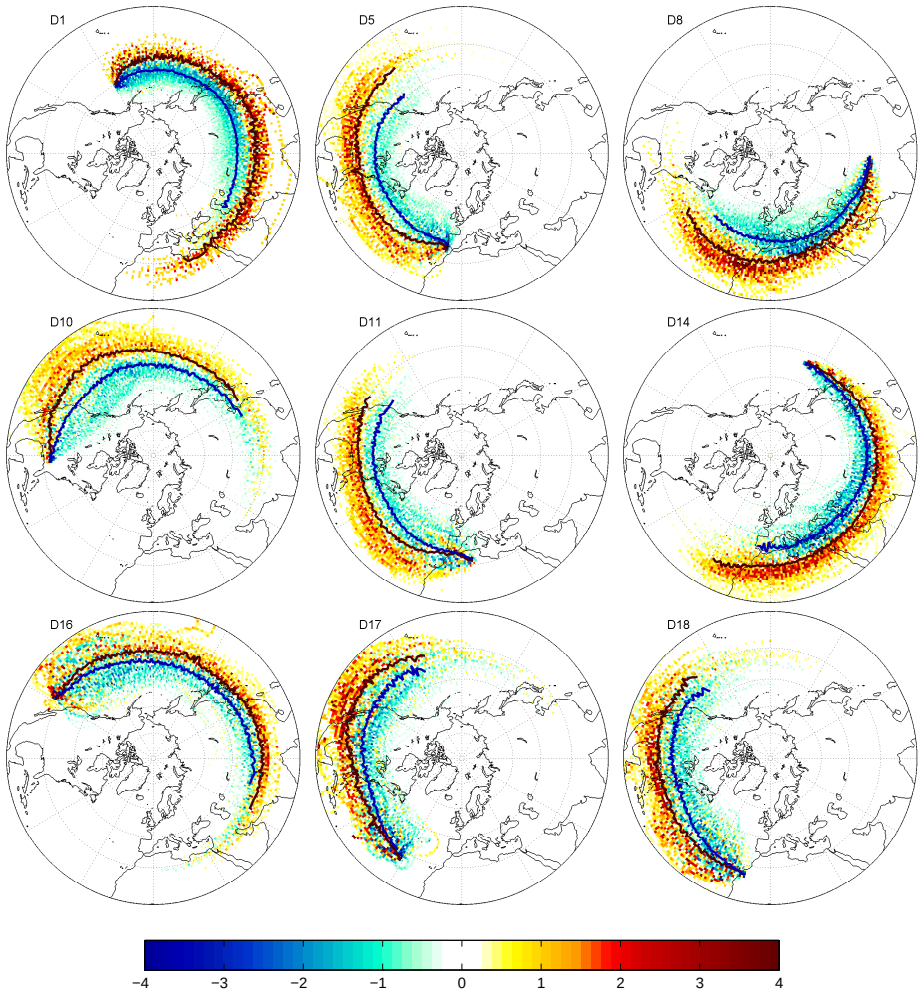

Fig. 2. Difference between DT and ST trajectory densities (DT - ST). Top to bottom rows show domains northward of the maximum occurrence of DTs, domains in the regions of maximum occurrence of DTs, and domains southward of the maximum of DTs. The differences are shown for 5-days back-trajectories. The solid lines represent the mean trajectory for ST cases (blue) and DT cases (red). The mean trajectories were calculated for bins crossed by, at least, 10% of events.

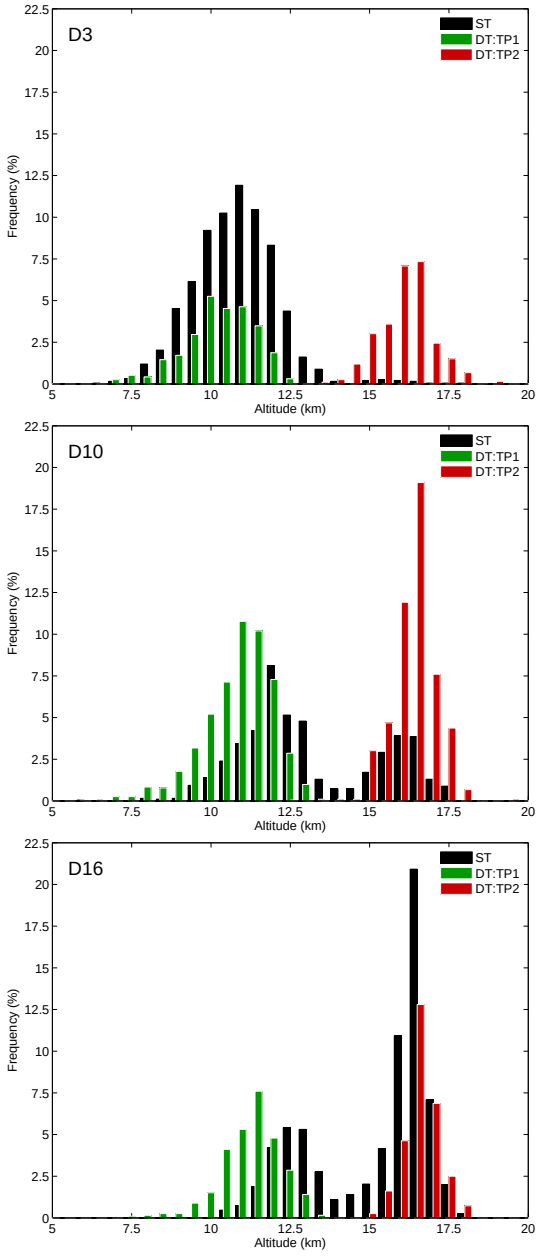

Fig. 3. Tropopause height distributions for ST cases (black bars) and DT cases (green bars for the first tropopause and red bars for the second tropopause). The sum of the black bars and the green bars (or red bars) gives the total frequency of 100%. The total frequencies of first tropopauses and second tropopauses is obviously equal.

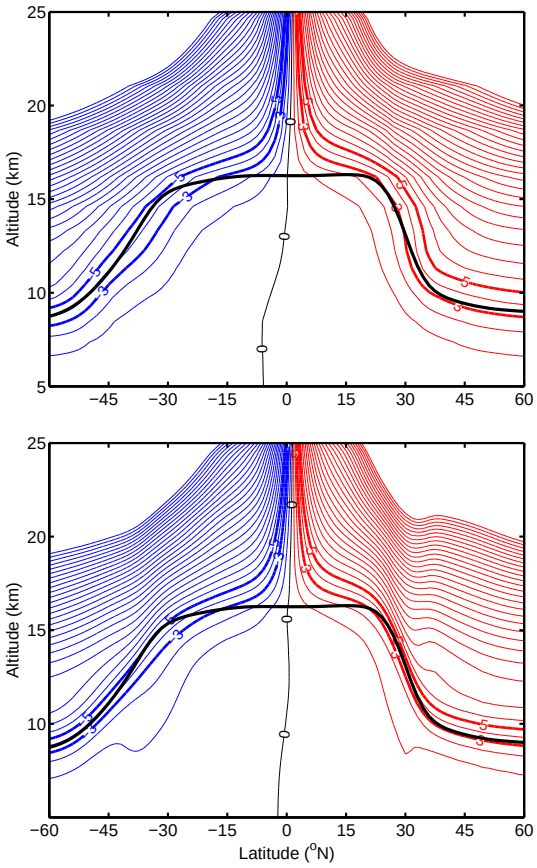

Fig. 4. January-mean, zonal-mean potential vorticity in (top) conventional vertical coordinates and in (bottom) tropopause-relative vertical coordinates. Contours were drawn at 1 PVU intervals, from 1 to 15 PVU in the NH, and -15 to -1 in the SH. The thick solid black line is the January-mean, zonal-mean height of the first tropopause. The altitude was calculated from the isobaric coordinates using $Z = 7 \times \log(p/p_s)$, where $p_s = 1000\,\mathrm{hPa}$.

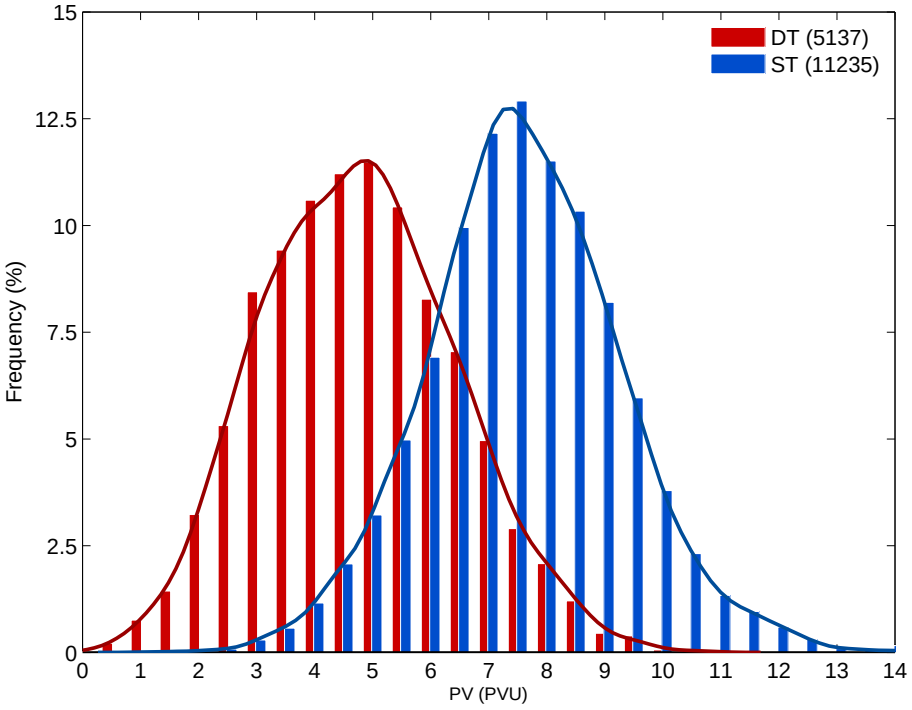

Fig. 5. Histograms and estimated PDFs of the mean potential vorticity for ST and DT events, considering all domains collectively.

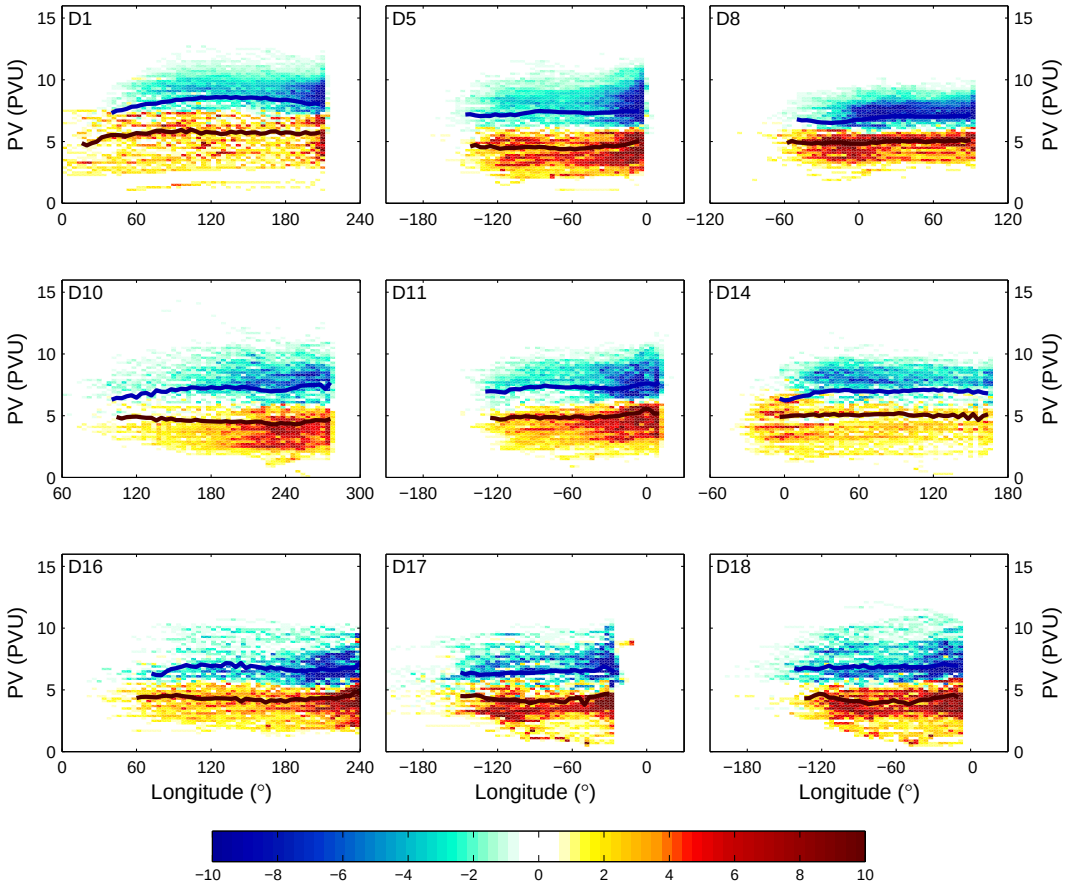

Fig. 6. Difference between DT and ST trajectory densities (DT - ST) in the longitude PV phase space, for the same domains represented in Fig. 2. The solid lines represent the mean trajectory for ST cases (blue) and DT cases (red). The mean trajectories were calculated for bins crossed by, at least, 25% of events.

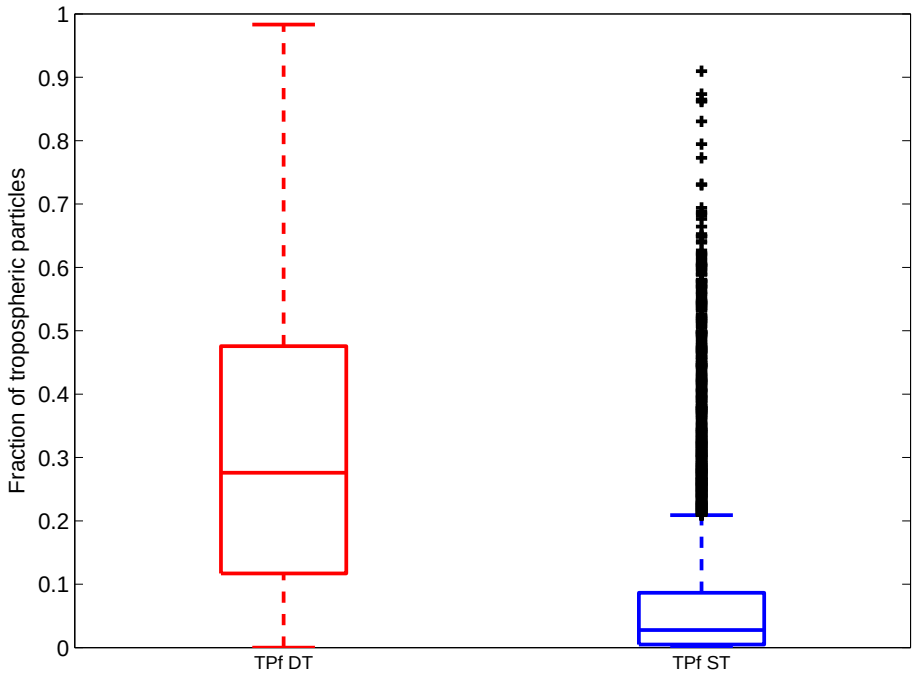

Fig. 7. Box plot diagrams of the mean fractions of tropospheric particles for ST and DT events, considering all domains collectively. Plus signs represent outliers, i.e. points at a distance from the 75^{th} percentile that is larger than 1.5 times the difference between 25^{th} and 75^{th} percentile.

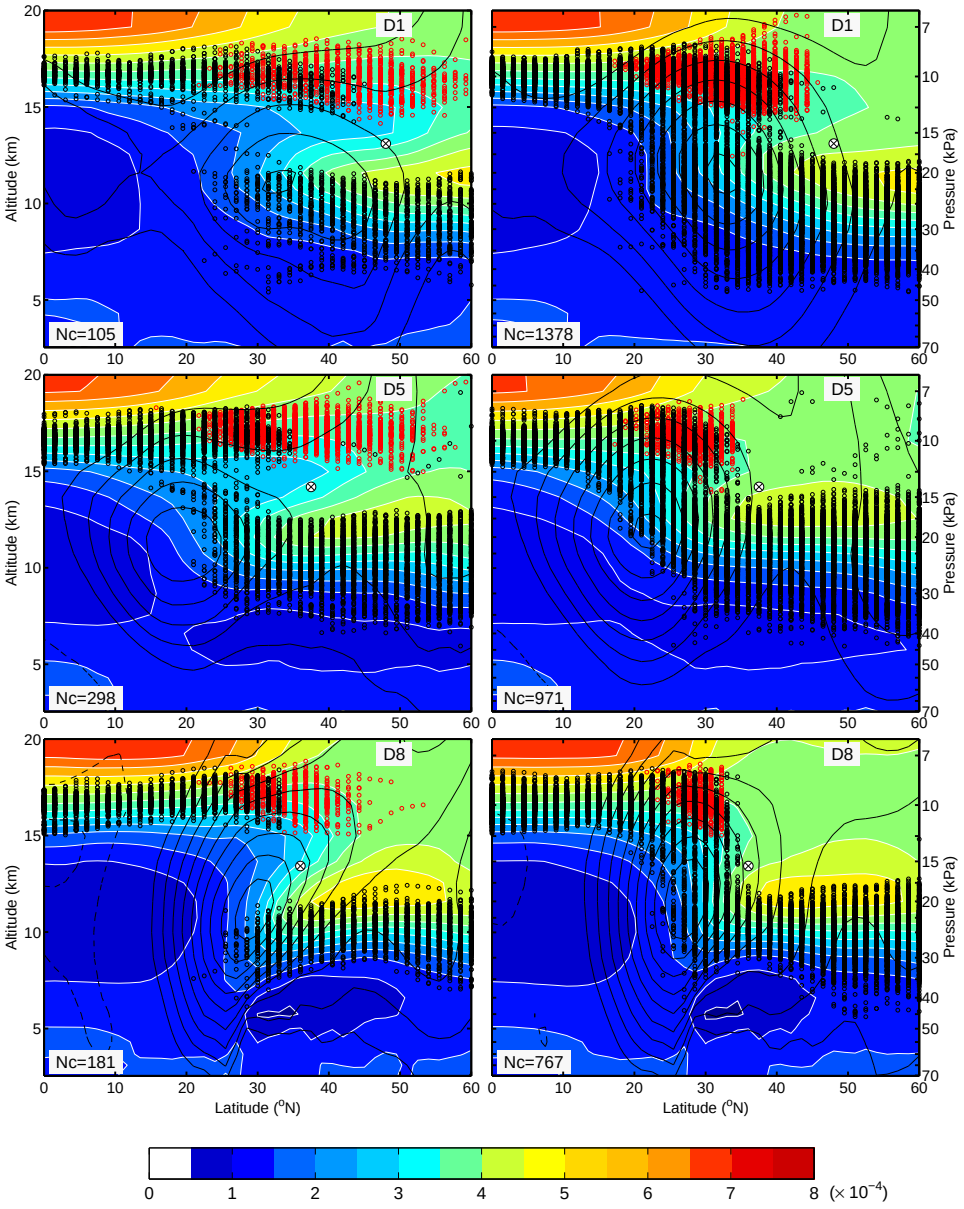

Fig. 8. Composites of static stability (N^2, colors filled, in s^{-2}) and zonal winds (contours) for DT (left column) and ST (right column) events. The composites were calculated along the meridian which passes in the center of the domain labeled in the right upper corner of each panel. The number of events (Nc) considered for the calculation of each composite is given in the left lower corner. Dashed black contours represent easterly wind and are drawn at $5\mathrm{ms}^{-1}$ intervals starting at $-5\mathrm{ms}^{-1}$. Solid black lines represent westerly wind and are drawn at $5\mathrm{ms}^{-1}$ intervals starting at $10\mathrm{ms}^{-1}$. Black dots represent the single or first tropopause, and red dots represent second tropopauses found equatorward of the tropopause break.

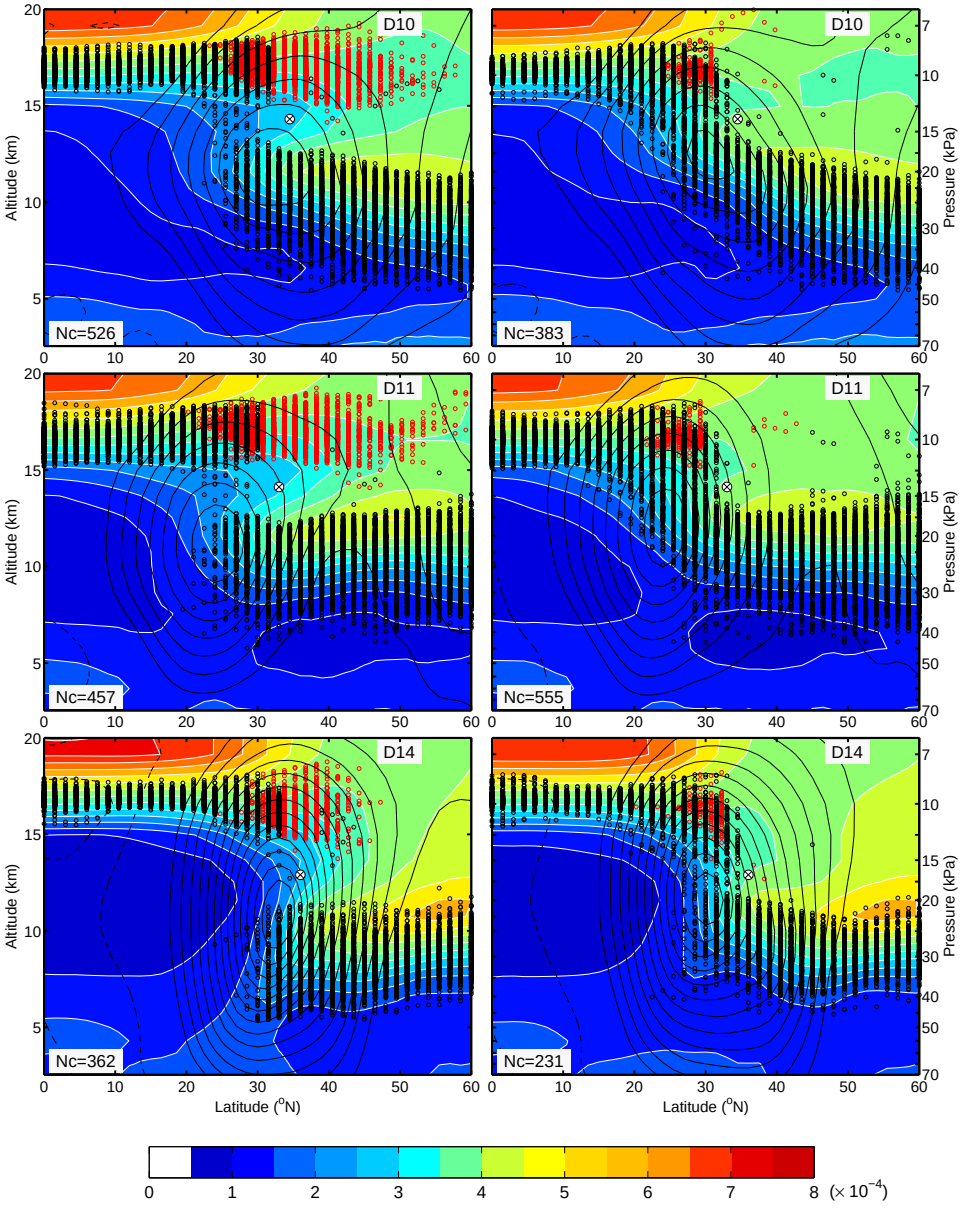

Fig. 9. As in Fig. 8 but for domains D10, D11 and D14.

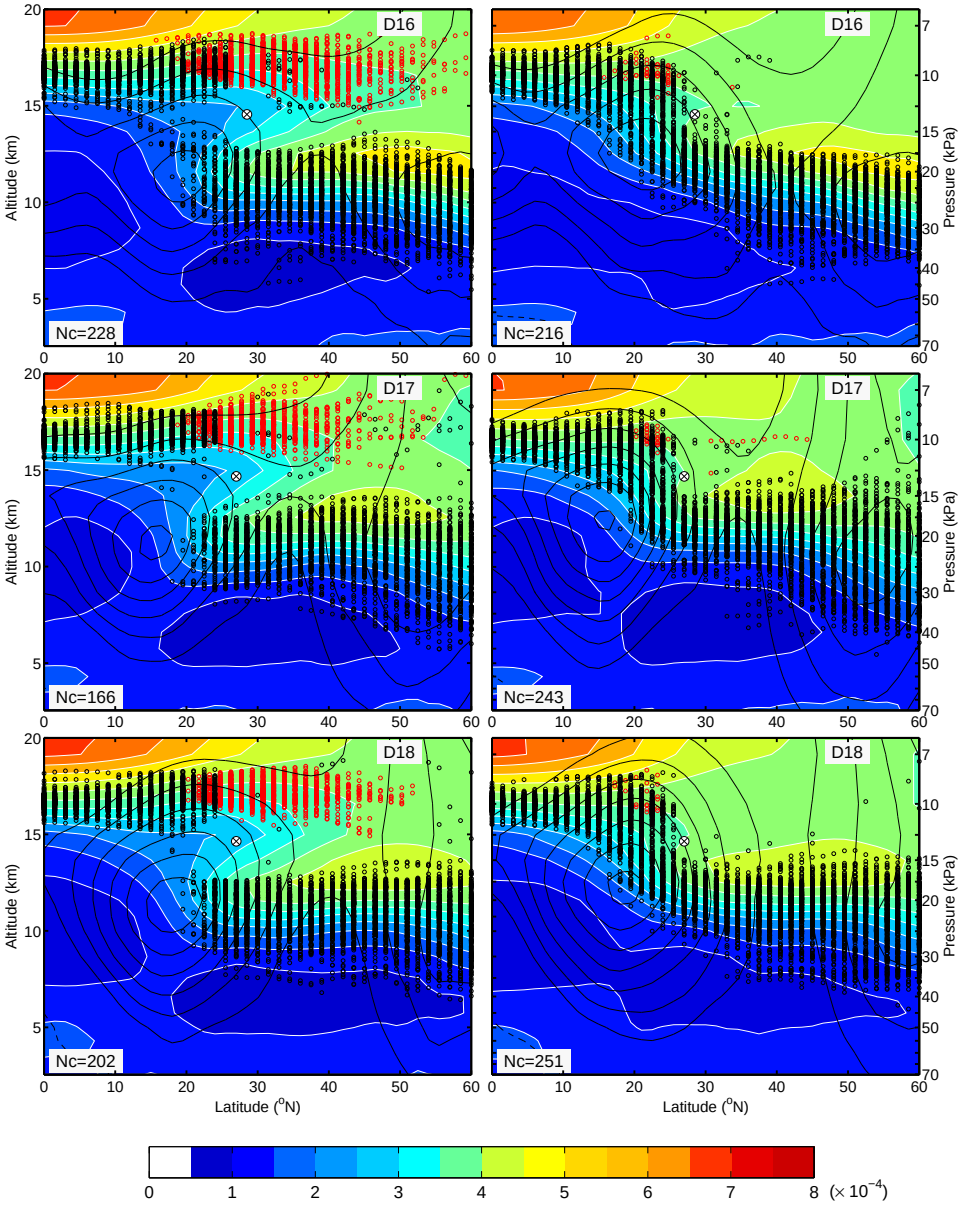

Fig. 10. As in Fig. 8 but for domains D16, D17 and D18.

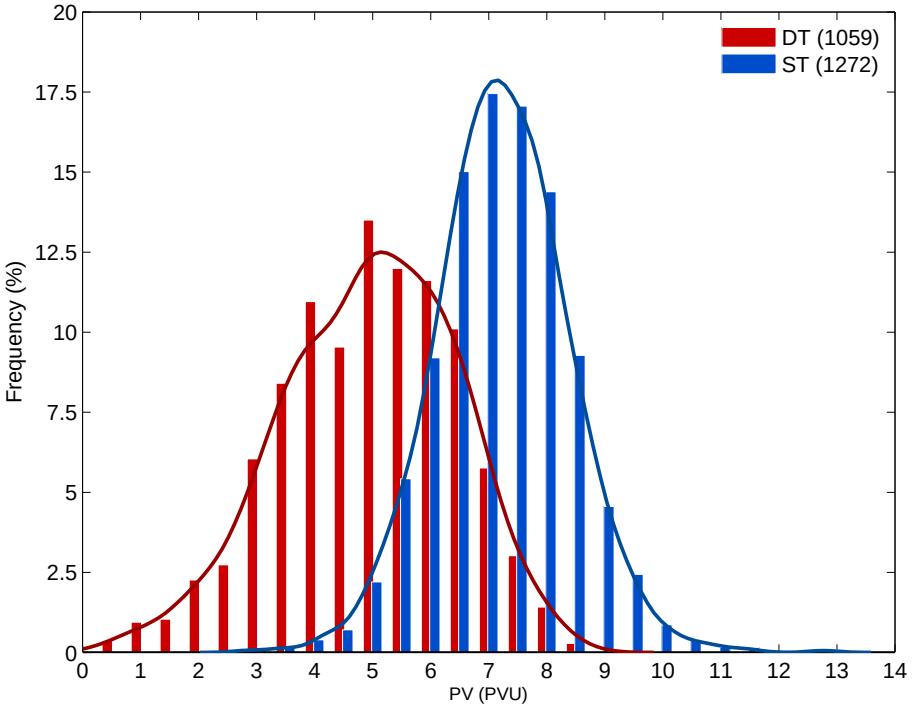

Fig. 11. Histograms and estimated PDFs of the mean potential vorticity for ST and DT events, considering the domains D8, D13, D14 and D20 collectively.